Angiogenesis QTL on Mouse Chromosome 8 Colocalizes with Differential β-Defensin Expression

Jason Smith,[1] Fang Liu,[1,2,3] Barbara Beyer,[1] Krista Morales,[1] Andrew Reilly,[1] Richard Cole,[1,2] and Bruce J. Herron[1,2]

[1]Wadsworth Center, New York State Department of Health, Albany, New York, USA; and [2]Department of Biomedical Sciences, School of Public Health, State University of New York at Albany, Albany, New York, USA

Identification of genetic factors that modify complex traits is often complicated by gene-environment interactions that contribute to the observed phenotype. In model systems, the phenotypic outcomes quantified are typically traits that maximize observed variance, which in turn, should maximize the detection of quantitative trait loci (QTL) in subsequent mapping studies. However, when the observed trait is dependent on multiple interacting factors, it can complicate genetic analysis, reducing the likelihood that the modifying mutation will ultimately be found. Alternatively, by focusing on intermediate phenotypes of a larger condition, we can reduce a model's complexity, which will, in turn, limit the number of QTL that contribute to variance. We used a novel method to follow angiogenesis in mice that reduces environmental variance by measuring endothelial cell growth from culture of isolated skin biopsies that varies depending on the genetic source of the tissue. This method, in combination with a backcross breeding strategy, is intended to reduce genetic complexity and limit the phenotypic effects to fewer modifier loci. We determined that our approach was an efficient means to generate recombinant progeny and used this cohort to map a novel s.c. angiogenesis QTL to proximal mouse chromosome (Chr.) 8 with suggestive QTL on Chr. 2 and 7. Global mRNA expression analysis of samples from parental reference strains revealed β-defensins as potential candidate genes for future study.

Key Words: genetics, mouse model, skin development

INTRODUCTION

Angiogenesis contributes complex diseases in mammals, including cancer, diabetes, psoriasis, and arthritis. Whereas abnormal vessel growth is not considered a primary etiology of these diseases, angiogenesis can mediate disease progression and is a potential route of therapeutic intervention.[1] Thus, a better understanding of the genetic factors that lead to differential vessel growth could identify disease modifiers and uncover novel avenues for treatment.

[3]Current address: Developmental, Stem Cell and Regenerative Biology, University of Pennsylvania, Philadelphia, Pennsylvania, USA. Address correspondence to: Bruce Herron, Center for Medical Science, NYS Dept. of Health, 150 New Scotland Ave., Albany, NY 12208, USA (E-mail: bruce.herron@health.ny.gov).

Abbreviations: AP3M2=adaptor-related protein complex 3, μ 2, B6=C57BL/6J, bp=base pair(s), CDC16=cell division cycle 16 homolog, Chr.=chromosome, CKAP2=cytoskeleton-associated protein 2, DEFB=defensin, β, EFNB2=ephrin-β2, EM=expectation-maximization, FVB=FVB/NJ, GC14=1700016D06Rik, LOD=logarithm of the odds (to the base 10), N2=second backcross generation, qPCR=quantitative PCR, QTL=quantitative trait loci, Scvg1=subcutaneous vessel growth quantitative trait loci 1, SNP=single nucleotide polymorphism, VPS36, vacuolar protein-sorting-associated protein 36

doi: 10.7171/jbt.15-2602-002

Many QTL have been identified by use of preclinical models, but the number of causal quantitative trait nucleotides discovered in these studies, while growing, remains limited. Numerous factors may contribute to these discrepancies, leading us to consider that the general approach for genetic complex trait analysis may have room for improvement. One potential limitation is the design of strategies that maximize observed phenotypic variance. The maximizing of variance in systems where only a few QTL are present is advantageous; however, phenotype complexity can negatively impact cloning the genetic contributions in a model where several QTL are present, or environmental factors modify outcomes. For example, whereas tumor susceptibility in mice can be mapped to multiple QTL,[2–5] the ultimate discovery of the underlying genes associated with tumor susceptibility can be limited by the interactions of multiple, small-effect QTL complicating downstream studies of individual loci. It is notable that when tumor susceptibilities are assigned to specific biologic functions, such as angiogenesis, in the context of increased tumor volume,[6,7] these subphenotypes are easier to attribute to candidate function and are typically controlled by fewer loci. This combination can lead to better identification of candidate genes and ultimately, the genetic basis of the disease.[8]

Growth and maintenance of blood vessels are mediated by many factors. VEGF is well studied and has been the focus

of therapies involving VEGF antibodies, such as antiangiogenesis treatment.[9] However, adverse side-effects of VEGF therapies[10] and its poor performance in specific tumor types indicate that additional pathways mediating vessel growth need to be discovered.

We have developed a skin biopsy assay to quantify early events in angiogenesis from neonatal and adult mice. Whereas this approach should be useful for discovering genes associated with vessel growth in skin-specific settings, such as wounding and psoriasis, the genes may also be associated with other diseases that have vessel growth abnormalities as a component of their etiology. We discovered a pattern of genetic heterogeneity in an angiogenic response that did not correlate with the patterns previously seen in *in vivo* angiogenesis studies.[11] This led us to consider that our *ex vivo* assay may identify novel genetic loci that influence vessel growth.

The defensins are a family of antimicrobial peptides that have been studied extensively. In addition to their role in innate immunity, defensin peptides are now implicated in additional physiologic processes, including increased expression in psoriatic lesions[12] and enhanced progenitor cell recruitment in vessel growth in tumors.[13,14]

We report here the mapping of VEGF-stimulated QTL associated with enhanced s.c. angiogenesis in FVB/NJ (FVB) mice. We mapped 2 suggestive QTL that overlap with previously identified angiogenesis QTL and a novel QTL on proximal mouse Chr. 8, supporting our hypothesis that more focused assays reduce genetic complexity in the QTL analysis. We have associated increased expression of 2 β-defensin family members within the confidence interval of our largest QTL and propose that they are good candidates for enhanced vessel growth.

MATERIALS AND METHODS

Mice were purchased from The Jackson Laboratory (Bar Harbor, ME, USA) or were bred at the Wadsworth Center (Albany, NY, USA). Animals were maintained on a 7 AM–7 PM, light-dark cycle with food and water available *ad libitum*. All procedures were approved by the Wadsworth Center Institutional Animal Care and Use Committee.

Angiogenesis assays were performed as described previously.[15] In brief, euthanized 3-day-old mice were sanitized and transferred to Eagle's minimal essential medium containing 1× Antibiotic-Antimycotic (Gibco, Life Technologies, Grand Island, NY, USA), or adult mice were plucked of all hair in the region to be assayed, and the region was sanitized, excised, and subsequently treated identical to the day 3 skin. A 2 × 2 cm full-thickness skin segment was removed from the dorsal flank between the shoulder blades, and 4, 2 mm circular biopsies were isolated. Biopsies were embedded, dermis side down, in Matrigel (BD Biosciences, San Jose, CA, USA) and warmed at 37°C in a tissue-culture incubator for 1 h. The biopsies were then fed endothelial cell basal medium 2 (Lonza, Basel, Switzerland) containing 20 ng/ml recombinant human VEGF (R&D Systems, Minneapolis, MN, USA), 2% fetal bovine serum (Sigma, St. Louis, MO, USA), 1× Antibiotic-Antimycotic, and 12.5 μg/μl chloramphenicol (Sigma). Cultures were maintained for 7 days, replacing the media, ~72 h after the start of culture.

Vessel Quantification

Matrigel-embedded explants were fixed for 1 h in at 25°C in 1× PBS containing 4% paraformaldehyde. Fixed samples were rinsed 3 times in 1× PBS and stained with 10 μg/ml Hoechst 33342 stain (Sigma) for 1 h. Biopsies were visualized with a light microscope (TE2000; Nikon, Melville, NY, USA), equipped for epifluorescence (2× 0.1 numerical aperture) at an excitation of 340–380 nm, with UV fluorescence collected at 435–485 nm. Image-Pro 6.2 (Media Cybernetics, Rockville, MD, USA) was used to collect a Z-series (70 μm step) with a charge-coupled device camera (Roper HQ; Roper Scientific, Trenton, NJ, USA). To set the extent of imaging steps, the upper and lower imaging focal limits were determined manually by visualization of the uppermost- and lowermost-stained nuclei in each biopsy. A maximum local contrast projection was generated from each image stack by Image-Pro 6.2 (Media Cybernetics).

Composite images were inspected for any growth irregularities, and irregular samples were excluded, including biopsies, in which vessels grew to the surface of the Matrigel and produced a monolayer on the surface of the gel plug or where the original biopsy was lost from the Matrigel. Fewer than 3% of the images were rejected by these criteria. Images exclusively of vessel growth were then generated by cropping the skin biopsy from the composite image by use of Photoshop CS3 (Adobe Systems, San Jose, CA, USA). The cropped 2-dimensional gray-scale projections were converted to black and white images and processed large spectral filters with a watershed routine to distinguish overlapping nuclei. The nuclei were then counted by use of a size-exclusion paradigm designed to count objects of a similar size (set area 2–50; Image-Pro 6.2; Media Cybernetics).

Mapping

Liver or skin tissue samples collected at the time of skin biopsy isolation were used for genomic DNA isolation with the Puregene DNA isolation kit, per the manufacturer's protocol (Qiagen, Valencia, CA, USA). Genomic DNA was then submitted to the Mutation Mapping and Developmental Analysis Project for single nucleotide polymorphism (SNP) analysis by use of a mapping panel showing good diversity between C57BL/6J (B6) and FVB.[16] A total of 509 informative SNPs between the parental strains were identified in this panel. Variation between groups of cultured skin biopsies (see Fig. 1)

were normalized by subtracting the average growth rate of 1 batch of samples [6–15 second backcross generation (N2) progeny/batch] from the average growth score of the individual (3–4 biopsies/animal), as described in Results.

Data Analysis

Mean normalized growth scores from N2 progeny, sex, and genotype information were determined for mapping analysis with R/qtl[17] by use of the J/qtl interface.[18] Single-interval QTL mapping was performed by use of the expectation-maximization (EM) algorithm or a Haley-Knott regression, treating the normalized data distribution as normal and by use of sex as an interactive covariate. Both algorithms produced similar results. Genome-wide significance levels were determined by permutation of the entire dataset by use of 5000 replicates. $P < 0.05$, genome wide, was considered to be significant.

Expression Analysis

Skin biopsies from B6 and FVB mice were cultured, as described above, for 5 days and rinsed twice in PBS at room temperature. Eight biopsies/RNA sample were scraped into 1 ml QIAzol (Qiagen) and homogenized immediately for RNA extraction, per the manufacturer's protocol. The aqueous phase was transferred to RNeasy mini columns and processed according to the manufacturer's protocol (Qiagen). RNA integrity was confirmed with the Agilent Bioanalyzer (Agilent Technologies, Santa Clara, CA, USA), which gave a RNA integrity number value of >8 for all samples.

One hundred micrograms of total RNA from 6 independent samples (3 each from B6 and FVB strains) was submitted to the Wadsworth Center Genomics Core Facility for microarray analysis. Samples were labeled with the Agilent Low RNA Input Linear Amplification Kit, according to the manufacturer's specifications (Agilent Technologies). Cy3-labeled cRNA targets samples were hybridized to Mouse GE 4X44K microarray (14868; Agilent Technologies); for all samples, dye-incorporation frequency was >15.

One-color-based gene-expression normalization and analysis were carried out by use of GeneSpring GX, Version 9.0. with the GeneChip Robust Multi-array Average algorithm. Data were filtered to focus analysis on samples with a present or marginal flag in at least 1 sample. An unpaired *t*-test (by strain) was performed to identify statistically significant differential expression (cutoff, $P < 0.05$), and false positives were minimized with a Benjamini-Hochberg multiple testing correction factor. Expression deferences are listed in Supplemental Table 1.

Quantitative PCR

Expression differences >2-fold that were under the 95% confidence interval of the Chr. 8 QTL were confirmed by quantitative PCR (qPCR) by use of PrimeTime qPCR Assays (Integrated DNA Technologies, Coralville, IA, USA). Primer designs are available in Supplemental Table 2. Primers were resuspended, according to the manufacturer's recommendations. First-strand cDNA was generated with random primers on 500 ng total RNA, isolated as described above. The manufacturer's protocol from the SuperScript III First-Strand Synthesis System (Invitrogen, Life Technologies, Carlsbad, CA, USA) was followed. cDNAs were diluted 10-fold, and real-time PCR was performed in a 7500 Real-Time PCR System with TaqMan Universal PCR Master Mix (Applied Biosystems, Life Technologies, Grand Island, NY, USA). Relative expression was determined by use of a standard curve generated from stock-pooled cDNA from all samples in the software provided by the manufacturer. Sample variance was normalized by expressing the results as a ratio of the target cDNA divided by the amount of 18s target in each sample.

RESULTS

Novel Method to Identify Angiogenesis QTL

Quantification of vessel growth was performed by use of our previously described approach to measure angiogenesis in subcutaneous microvessels.[15] This model is designed to uncover differences in the early steps of angiogenesis, including processes, such as endothelial cell sprouting and proliferation. By focusing on a short-term window, we could also discover factors responsible for vessel growth in established vasculature (*e.g.*, tumor angiogenesis) but with less impact from environmental variance as a result of the limited time course of the assay. Skin biopsies are isolated from postnatal animals (3-day-old mice in this study) that are embedded in Matrigel and grown in a media that encourages endothelial cell growth from tissue biopsies with the vessel-specific growth factor VEGF. After 7 days of culture, endothelial cells are quantified by fixing the *ex vivo* culture, staining with a DNA-specific dye, and counting the total number of endothelial cells that grew into the Matrigel by use of a semiautomated method.[15] A caveat of this approach is that whereas we have performed extensive controls of this assay to ensure that most, if not all, cells growing from the culture are endothelial [branching structures, staining with endothelial-specific markers (data not shown)], it is not practical to do so in larger-scale studies with hundreds of individuals. Cultures from B6 animals exposed to 20 ng/ml VEGF grow an average of 1150 cells from 2 mM punch biopsies, whereas FVB biopsies are more proliferative with an average of 1785 cells (**Fig. 1A**), which is consistent with our previous reports.[15]

Variations in Endothelial Cell Growth Are Influenced by Genetic and Environmental Factors

Whereas B6 consistently showed low angiogenic response compared with simultaneously cultured FVB biopsies, we also observed intrastrain variation growth between B6 cultures

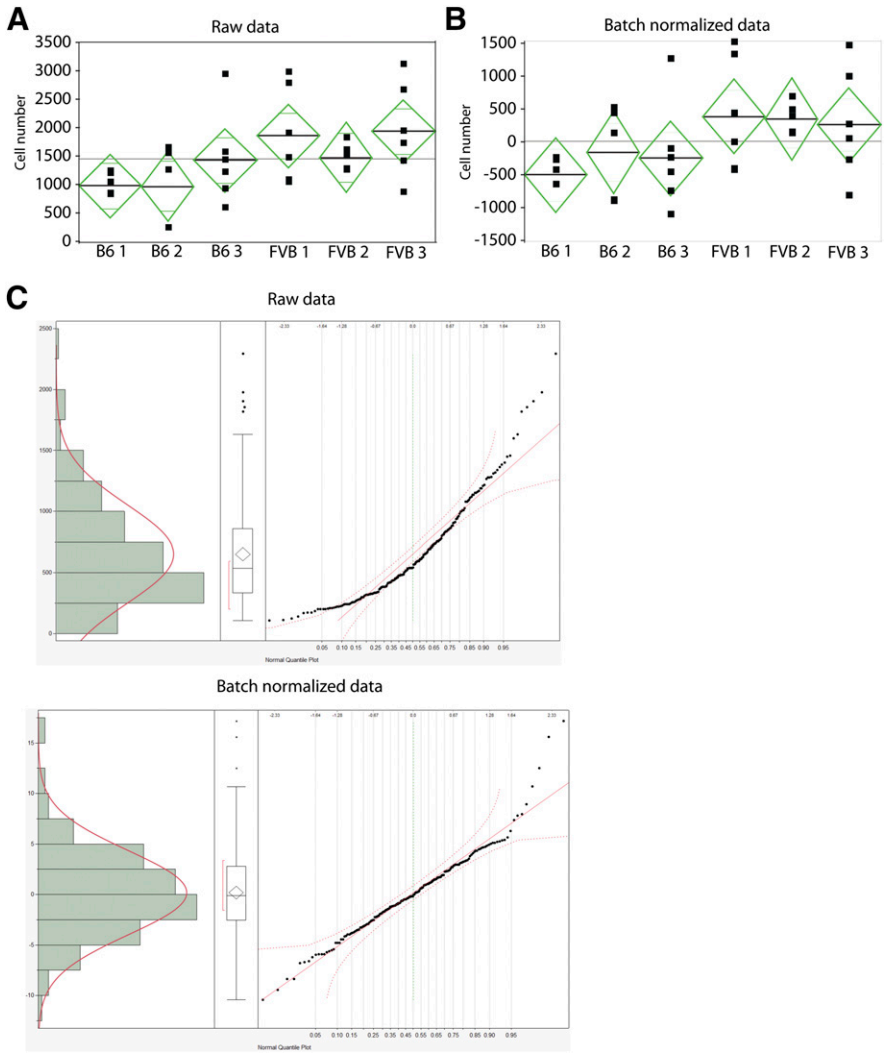

FIGURE 1

Normalization of batch-specific effects in s.c. angiogenesis assay. *A*) Comparison of raw data from 3 groups of B6 and FVB cultured on separate dates (B61 and FVB1 = batch 1, etc.). *B*) Comparison of batch mean normalized data. Note the increased concordance between B6 samples from different batches, whereas the relative responses within a batch are consistent with those in *A*. Gray line across each box deliniates composite mean for all samples; black lines within diamonds identify mean for each group, whereas diamonds illustrate the confidence interval for each group. Black dots represent the average response for individuals (average growth response of 4 biopsies from each animal) within a group. *C*) Histogram showing of distribution of cell counts from individuals in the N2 cross as the raw result (upper) and after normalization (lower) producing a more normal distribution, as shown by the accompanying normal quantile plots.

performed at different dates (**Fig. 2A**). These environmental variations are likely a result of differences in culture conditions, such as the small differences in the lot of Matrigel and other components of the growth media that may vary between assays. For example, when cohorts of B6 mice were processed on separate dates, there were differences in average growth rates between sets (B6-1 compared with B6-2; Fig. 1A). However, when B6 and FVB were compared within sets from the same date (*i.e.*, B6-1 compared with FVB-1, etc.), we observed relative growth differences between them. We calculated the heritability to be 0.38 by use of the raw cell count data between B6 and resulting in a significance level of $P < 0.008$. Thus, whereas significant differences were present, interbatch environmental variance is predicted to reduce QTL detection power when comparing mice derived from multiple batches.

To minimize the impact of environmental variance, we used a normalization approach that subtracted the mean vessel growth for batch of simultaneously cultured biopsies from the average score of each individual. The subtraction of the average growth response of each animal (determined from 4 biopsies/individual) produced the batch-normalized value, where the relative growth responses centered around 0, rather than the average growth for that group (Fig. 1B). This normalization method reduced intrastrain variance, increasing the heritability to 0.41 between B6 and FVB ($P < 0.006$; Fig 1B). Notably, when similar normalizations were applied to our backcross cohort (see Fig.1C and below), histograms and normal quantile plots showed a shift from a non-normally skewed dataset to a more normal distribution, resulting in a Shapiro-Wilk value of 0.96 ($P < 0.0006$).

Mapping Analysis

In addition to normalizations intended to reduce environmental variance, we reduced the complexity of our genetic analysis by use of a backcross-breeding scheme. This was initiated based on our previous work showing that [B6XFVB]F1 vessel growth rates were similar to FVB/FVB.[15] A [B6XFVB]F1 × FVB backcross was used to generate 174 N2 animals that were

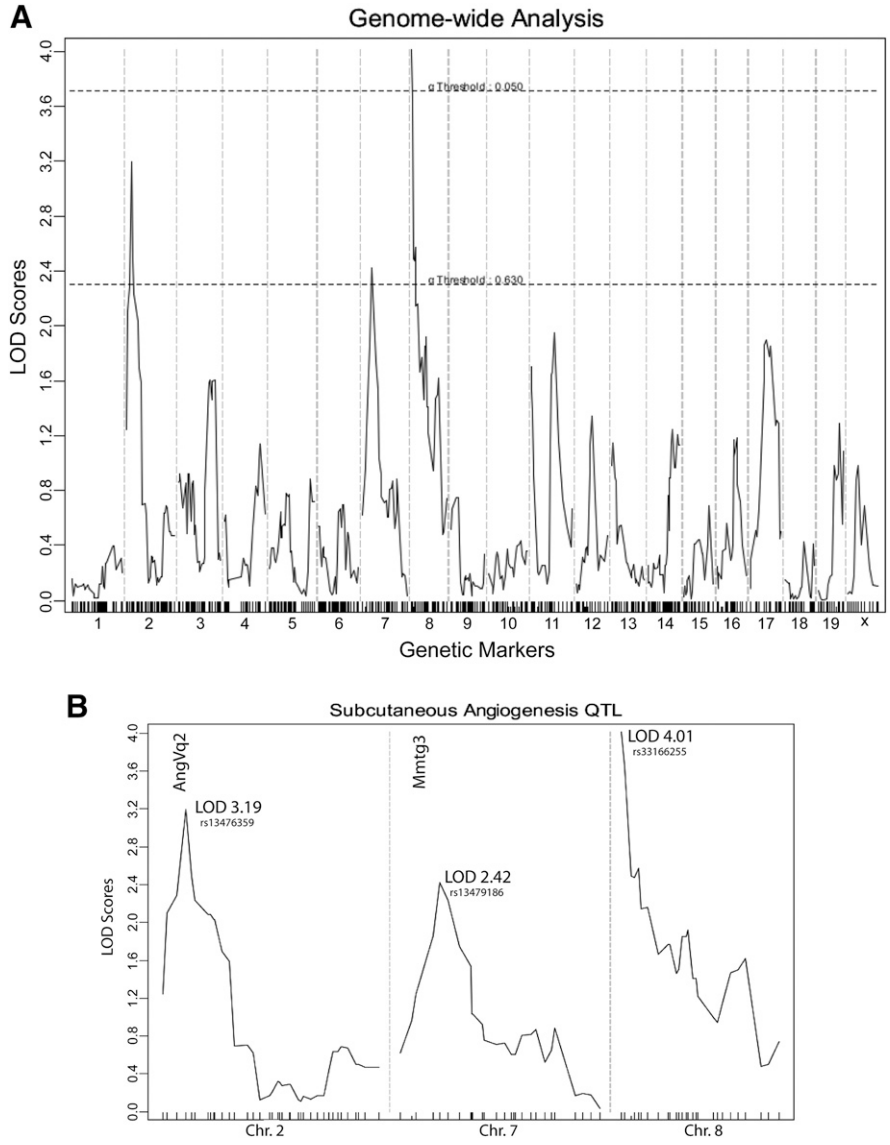

FIGURE 2

Mapping analysis of s.c angiogenesis QTL. *A*) Genome-wide representation of mapping results are shown with centromeres to the right on each successive Chr. with the logarithm of the odds (to the base 10; LOD) score on the *y*-axis and the markers on the *x*-axis. Dashed horizontal lines delineate suggestive significance (0.63 LOD = 2.25; lower line) and significance (0.05 LOD = 3.70; upper line). *B*) Expanded view of Chr. 2, 7, and 8. Maximum LOD is indicated for peak effect, and the approximate position of previously detected angiogenesis QTL is indicated with vertical text. AngVq2, angiogenesis by VEGF QTL 2; Mmtg3, modifier of mammary tumor growth 3.

evaluated for vessel growth. We used 3-day-old animals in this study to minimize the environmental variance that is present in older mice that are associated with changes in skin thickness and vessel density during anagen hair growth. Average vessel growth score from 4 biopsies/N2 animal was normalized against batch averages, and genomic DNA was hybridized to a genome-wide mapping panel that was designed to maximize informative content between B6 and other domesticus strains.[16] Genotype and phenotype data were correlated by use of R/QTL with the use of the sex of individuals as an interactive covariate implementing the EM.[17] As shown in Fig. 2, a single QTL, reaching a genome-wide significance of $P < 0.05$ (based on 5000 permutations of the dataset), was detected on proximal mouse Chr. 8, and 2 suggestive QTL ($P > 0.63$) were detected on Chr. 2 and 7. Whereas the Chr. 8 locus has not been identified in previous studies mapping angiogenesis QTL in mice, the Chr. 2 locus is in the vicinity of AngVq2, a corneal angiogenesis QTL previously detected in this region. The suggestive QTL on Chr. 7 was in the same region as Mmtg3, a QTL reported to modify tumor vessel growth in FVB (Fig 2B).[19,20] We have provisionally named the Chr. 8 QTL s.c. vessel growth QTL 1 (Scvg1), in accordance with nomenclature guidelines (see Section 2.10.1 in http://www.informatics.jax.org/mgihome/nomen/gene.shtml).

Interactions between Contributing Genetic and Environmental Factors

We then looked for additional sources of variation in our model by determining how the sex affects an individual, which had a small but nonsignificant impact on our cohort with males, showing a slightly higher average growth response than females (data not shown). We found that male and female

groups had opposing affects when we compared their average effects at the marker peak of the Chr. 2 locus. Alternatively, the Chr. 7 effect plots showed differences in male N2 but no differences in female progeny. Finally, Scvg1 effects were comparable in both sexes (**Fig. 3**), indicating that Scvg1 effects were independent of sex.

To define further the relationships between genetic factors that enhance vessel growth, we looked for genetic interactions are between 2 QTL with a pair-wise mapping analysis. None of these interactions was large enough to achieve significance in a cross of this size, but the top 2 interactions between autosomes were detected among the 3 QTL detected in our primary scan on Chr. 2 and Chr. 7 (full LOD 6.7) and between Chr 2 and Scvg1 (full LOD 7.8). Closer examination of these interactions (**Fig. 4**) in effect plots shows that the interactions are principally additive, indicating that these loci behave in an independent manner.

Candidate Locus Screen

To identify potential candidate genes, we surveyed the first 23 million base pairs (bp) of sequence between B6 and FVB by use of the mouse genomes project SNP query tool (http://www.sanger.ac.uk/sanger/Mouse_SnpViewer/rel-1410; see Supplemental Table 2).

We compared all coding missence, splice, and deletion/insertion mutations that could impact the function of gene on proximal mouse Chr. 8. No SNPs of this nature were detected in the first 15 million bp of Chr. 8, although many noncoding SNPs were present (not shown) between these strains. There was an increase in coding SNP occurrence from 15 to 23 million bp, which was the extent of the confidence interval for Scvg1. Among the potential mutations of interest were several missence mutations in defensin genes, along with a few in the microcephaly gene 1 (Mpch1), a gene that when mutated in mice, increases the level of corneal vessels in homozygous mutants (see https://www.mousephenotype.org/data/genes/MGI:2443308); however, it is not clear if this targeted Mcph1 mutation has off-target effects on the angiopoietin 2 gene that is within 100 kb of the Mcph1-targeted allele. Further study of this protein and its role in vessel growth are planned.

Next, we generated expression profiles from FVB- and B6-cultured skin biopsies by isolating mRNA for hybridization to Agilent Whole Human Genome Oligo Microarray Kit.[21] More than 900 genes were significantly altered between B6 and FVB (1.8-fold or greater differential expression after multiple testing correction; $P < 0.05$; Supplemental Table 1). To focus on differentially expressed genes that may be responsible for the variance attributed to Scvg1, we limited our study to differentially expressed genes under the 95% confidence interval of this locus. Among the candidates, 2 members of the defensin cluster on proximal mouse Chr. 8 were differentially

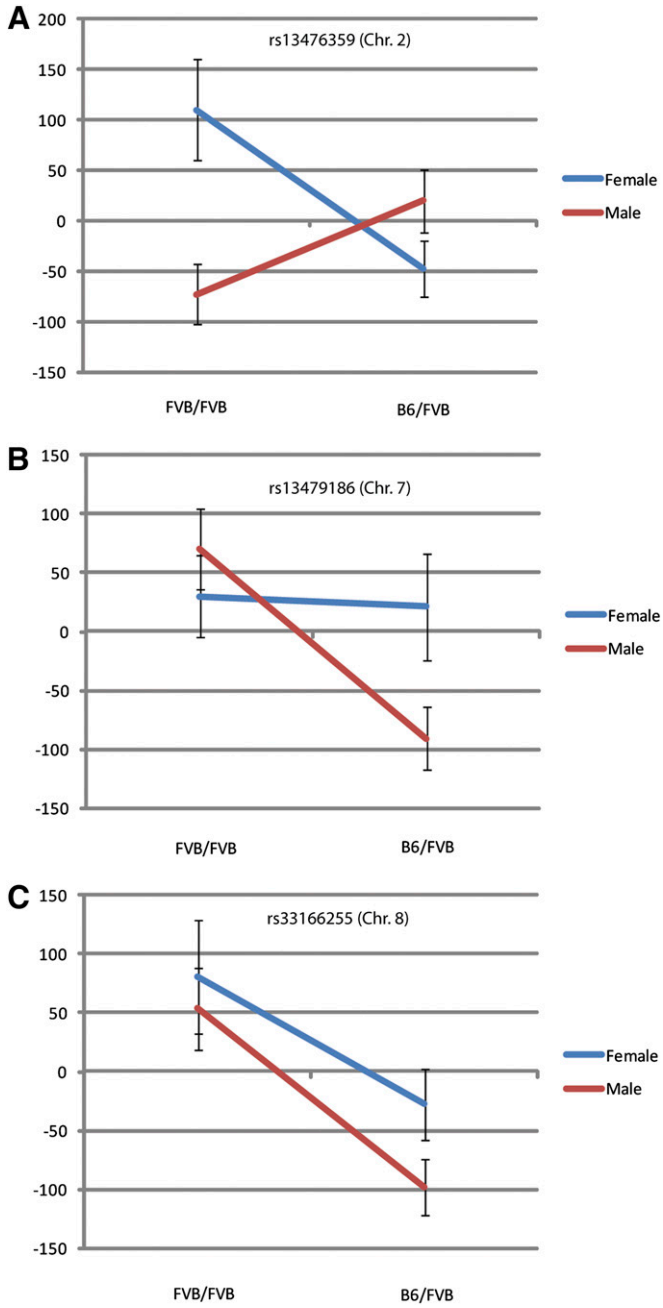

FIGURE 3

A) Effect plots for 3 QTL showing the impact of sex of individuals on vessel growth. Plots were generated in R/qtl by use of the markers with the maximum significance on (*A*) Chr. 2 (rs13476359), (*B*) 7 (rs13479186), and (*C*) 8 (rs33166255), with female samples indicated by a blue line and male samples indicated by a red line. Error bars indicate SEM.

expressed [defensin, β 1 and 14 (DEFB1 and DEFB14)], as were the 1700016D06Rik (GC14), cell division cycle 16 homolog (CDC16), ephrin-β2 (EFNB2), cytoskeleton-associated protein 2 (CKAP2), vacuolar protein-sorting-associated protein 36 (VPS36), and adaptor-related protein complex 3, μ 2 (AP3M2; see Supplemental Table 1).

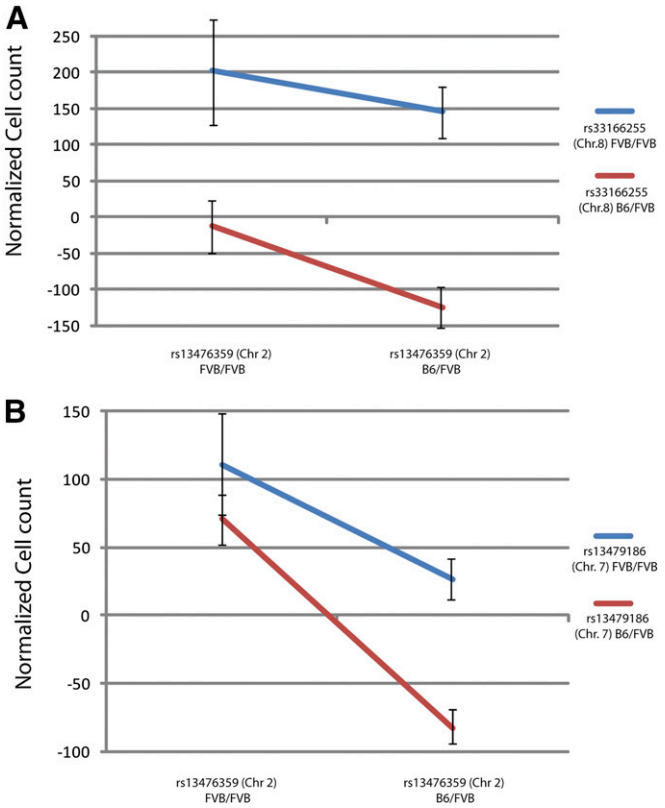

FIGURE 4

A) Effect plots showing interaction between Chr. 2 locus and subcutaneous vessel growth QTL 1 (Scvg1) and (*B*) Chr. 2 and Chr. 7. The Chr. 2 effects for the FVB/FVB genotypes and the B6/FVB genotypes are indicated on the *x*-axis, whereas the interaction of the Chr. 2 genotypes with the Chr. 8 genotypes (blue, FVB/FVB; red, B6/FVB) and Chr. 7 genotypes are shown by the distance and slope between the lines, respectively. Note the near-parallel lines indicate an additive interaction between these QTL.

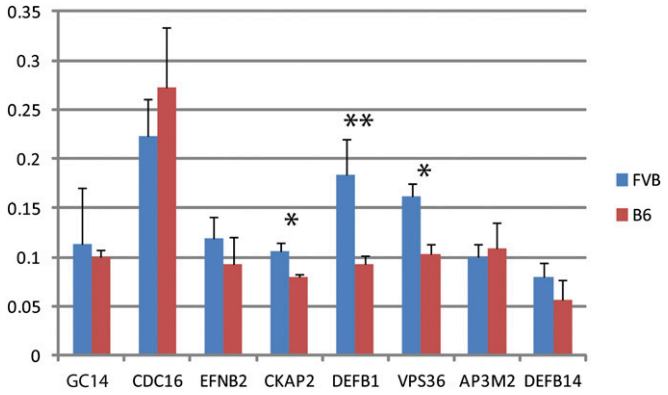

FIGURE 5

Real-time qPCR of Scvg1 candidate genes. Relative expression levels of GC14, CDC16, EFNB2, CKAP2, DEFB1, VPS36, AP3M2, and DEFB14. Relative amounts of mRNA were determined, as described in Materials and Methods and are expressed as a ratio of 18S RNA in that sample. $*P < 0.05$; $**P < 0.01$.

To confirm differential expression real-time qPCR was performed on the 8 candidates deemed significantly different in the array by use of independent RNA samples from similarly cultured skin biopsies. As shown in **Fig. 5**, only Defb1, Ckap2, and VPS36 reproduced significant expression differences in independent triplicate skin biopsies from B6 and FVB animals (Fig. 5).

DISCUSSION

The discovery of genetic loci that modify vessel growth has been an area of increasing interest in clinical and preclinical research.[22–27] Whereas the genes behind these loci are potentially powerful tools for risk assessment and therapeutic intervention, angiogenesis is intimately associated with tissue development and survival, limiting our ability to identify genetic factors regulating vessel growth by use of gene-targeting approaches.[28] However, the use of model systems by us and others[19,20] in various tissue-specific assays, by use of vessel growth as a complex trait, is beginning to find novel genes that also control vessel growth.[23]

Whereas our goal with this angiogenesis model was to identify specifically factors that mediate vessel growth, there are caveats associated with this approach. Despite the use of several methods to ensure that the outgrowth from skin biopsies was predominantly endothelial cells, it was not practical to apply these methods to our mapping cohort. Moreover, as a number of skin-resident cell populations can express markers typically thought to be markers for endothelial cells (*e.g.*, cadherin 5 tie 2, etc.), the more conclusive phenotypic evidence used in other angiogenesis quantification methods (*e.g.*, blood-filled capillaries) is not available for our model. Thus, it was satisfying to observe that QTL from our model overlap with these other studies of angiogenesis, supporting our approach to discover s.c. angiogenesis modifiers.

Consistent with our predictions, the s.c. angiogenesis model, which is designed to follow early events in angiogenesis with less impact from environmental variance, found fewer significant QTL than previous studies. The presence of suggestive QTL that overlapped with these other models also strengthened the potential that our approach bridges the connection between simple culture models of angiogenesis and the more complex to *in vivo* models.[19,20] It is not clear why these overlapping, smaller affect loci did not achieve the genome-wide significance reported in the previous studies, but the differences may lie in the short time-frame of our assay or possibly that we measured angiogenesis in both sexes.

It is less notable that our findings support a model where a combination of shared and unique genetic loci modifies angiogenesis in different vessel beds. Whereas corneal and s.c. angiogenesis may share QTL on mouse Chr. 2,[20] stronger novel effects were detected on Chr. 8 in the s.c. model. These

differences could be related to variation in the polymorphisms carried by different strains, but poor correlation between strain data of the *ex vivo* and *in vivo* models has been reported by us previously,[15] suggesting that tissue-specific genetic modifiers are likely also present.

Additionally, a tumor study performed in FVB has implicated proximal mouse Chr. 7 in a vessel density QTL between I/nJ and FVB,[19] a region that was also identified as a suggestive QTL in our study. These data indicate that an FVB allele on proximal Chr. 7 mediates angiogenesis in multiple assays, supporting the need for a more detailed analysis of this region. These studies await additional data to confirm the significance of this region. Whereas corneal angiogenesis may be driven by coat-color genes on mouse Chr. 7,[23] no correlation between coat color and angiogenesis was seen in our work (data not shown). However, without knowing the mechanisms that modify both of these systems, it is difficult to speculate on the basis, if any, of their relationship.

As the largest effect identified in this work was a novel QTL, discovered on proximal Chr. 8, exclusive to our s.c. angiogenesis model, it is compelling to consider that the underlying genetic defect is within a skin-specific factor. The skin harbors a variety of systems that are primarily expressed in this organ, which mediate wound healing, immune response, and thermoregulation. Whereas all of these processes could contribute to vascular development, the challenge to determine which gene(s) may mediate these phenomena rests upon finding an appropriate system to evaluate contributions.

As most polymorphisms between FVB and B6 are intergenic, an initial hypothesis was to consider that one of these polymorphisms altered the expression of a candidate gene that led to the differential growth phenotype of Scvg1. We used genome-wide expression analysis, comparing transcript levels of B6- and FVB-cultured biopsies. Whereas several interesting pathways were present in the genome-wide data, our focus here was specifically on the genes under the 95% confidence interval.

Expression differences in EfnB2 were 1 of the more compelling genes detected in our array studies. EfnB2 has been implicated in the spouting stages of dermal angiogenesis and lymphagenesis, processes that would be readily observed in our *ex vivo* angiogenesis model.[29] However, our confirmatory qPCR assay showed smaller differences in EfnB2 that were not significantly different between B6 and FVB, and sequencing of the EfnB2 open-reading frame revealed no coding differences that would lead to differential vessel growth. The original difference seen in the array may be a spurious result or could result from an over-representation of arterial versus venous vessel growth in the samples assayed, as mature s.c. vessels express EfnB2 and Ephb4, respectively.[30]

Of the 3 candidates that were altered significantly in array and confirmatory qPCR expression assays, Defb1 is an excellent candidate for future study. There is considerable evidence from multiple sources showing a role for defensins in angiogenesis. These small antimicrobial peptides have 2 subfamilies: the α-defensins, secreted mainly by neutrophils in intestinal Paneth cells,[31] are antiangiogenic and have been implicated in developmental and pathogenic angiogenesis;[32,33] alternatively, the epithelially expressed β-defensins have been shown to be proangiogenic.[13,14]

The Defb29 protein was shown to cooperate with VEGF to promote vasculogenesis by recruitment of dendritic precursor cells to tumors that would subsequently differentiate into endothelial-like lineages via VEGF-dependent pathways.[13] More recently, Defb14, a gene that was differentially expressed in our array data that is in the same cluster as Defb1, was shown to be expressed in mouse fibrosarcoma tissue, and this expression attracted CCR6+ lymphocytes.[14] Whereas Defb14 expression was not significant in our confirmatory qPCR, the direction of expression change was consistent between assays, and Defb1 was significantly, differentially expressed between B6- and FVB-cultured biopsies.

Based on these preliminary results, we propose that Defb1 may also play a proangiogenic role in s.c. vasculature. This conclusion would be the first evidence that genetic heterogeneity in defensin expression can contribute to differential vessel growth. A more detailed study of Defb1 and its impact on Scvg1 activity are warranted.

In conclusion, we have discovered a novel locus that alters the angiogenic potential of s.c. vasculature. Identification of the underlying mutations that lead to this unique complex trait should reveal mechanisms that are involved in early vessel growth and may uncover novel targets for therapeutic angiogenesis in the future.

ACKNOWLEDGMENTS

The authors thank the Wadsworth Center Advanced Light Microscopy Core, Advanced Genomics Technologies Core, and the Wadsworth Center Veterinary Sciences Program for their support in the completion of this research. Research reported in this publication was supported by the National Institute of Arthritis and Musculoskeletal and Skin Diseases of the U.S. National Institutes of Health (NIH) under Award Number R01AR054828. The content is solely the responsibility of the authors and does not necessarily represent the official views of NIH. No financial conflicts are disclosed.

REFERENCES

1. Folkman J. Tumor angiogenesis: therapeutic implications. *N Engl J Med* 1971;285:1182–1186.
2. Liu P, Wang Y, Vikis H, Maciag A, Wang D, Lu Y, Liu Y, You M. Candidate lung tumor susceptibility genes identified through whole-genome association analyses in inbred mice. *Nat Genet* 2006;38:888–895.
3. Wang M, Lemon WJ, Liu G, Wang Y, Iraqi FA, Malkinson AM, You M. Fine mapping and identification of candidate pulmonary adenoma susceptibility 1 genes using advanced intercross lines. *Cancer Res* 2003;63:3317–3324.

4. Devereux TR, Kaplan NL. Use of quantitative trait loci to map murine lung tumor susceptibility genes. *Exp Lung Res* 1998;24: 407–417.
5. Nagase H, Bryson S, Cordell H, Kemp CJ, Fee F, Balmain A. Distinct genetic loci control development of benign and malignant skin tumours in mice. *Nat Genet* 1995;10:424–429.
6. Lancaster M, Rouse J, Hunter KW. Modifiers of mammary tumor progression and metastasis on mouse chromosomes 7, 9, and 17. *Mamm Genome* 2005;16:120–126.
7. Le Voyer T, Lu Z, Babb J, Lifsted T, Williams M, Hunter K. An epistatic interaction controls the latency of a transgene-induced mammary tumor. *Mamm Genome* 2000;11:883–889.
8. Crawford NP, Qian X, Ziogas A, Papageorge AG, Boersma BJ, Walker RC, Lukes L, Rowe WL, Zhang J, Ambs S, Lowy DR, Anton-Culver H, Hunter KW. Rrp1b, a new candidate susceptibility gene for breast cancer progression and metastasis. *PLoS Genet* 2007;3:e214.
9. Grothey A, Galanis E. Targeting angiogenesis: progress with anti-VEGF treatment with large molecules. *Nat Rev Clin Oncol* 2009;6:507–518.
10. Meadows KL, Hurwitz HI. Anti-VEGF therapies in the clinic. *Cold Spring Harb Perspect Med* 2012;2:pii: a006577.
11. Rohan RM, Fernandez A, Udagawa T, Yuan J, D'Amato RJ. Genetic heterogeneity of angiogenesis in mice. *FASEB J* 2000; 14:871–876.
12. Jansen PA, Rodijk-Olthuis D, Hollox EJ, Kamsteeg M, Tjabringa GS, de Jongh GJ, van Vlijmen-Willems IM, Bergboer JG, van Rossum MM, de Jong EM, den Heijer M, Evers AW, Bergers M, Armour JA, Zeeuwen PL, Schalkwijk J. Beta-defensin-2 protein is a serum biomarker for disease activity in psoriasis and reaches biologically relevant concentrations in lesional skin. *PLoS ONE* 2009;4:e4725.
13. Conejo-Garcia JR, Benencia F, Courreges MC, Kang E, Mohamed-Hadley A, Buckanovich RJ, Holtz DO, Jenkins A, Na H, Zhang L, Wagner DS, Katsaros D, Caroll R, Coukos G. Tumor-infiltrating dendritic cell precursors recruited by a beta-defensin contribute to vasculogenesis under the influence of VEGF-A. *Nat Med* 2004;10:950–958.
14. Röhrl J, Huber B, Koehl GE, Geissler EK, Hehlgans T. Mouse β-defensin 14 (Defb14) promotes tumor growth by inducing angiogenesis in a CCR6-dependent manner. *J Immunol* 2012; 188:4931–4939.
15. Liu F, Smith J, Zhang Z, Cole R, Herron BJ. Genetic heterogeneity of skin microvasculature. *Dev Biol* 2010;340: 480–489.
16. Moran JL, Bolton AD, Tran PV, Brown A, Dwyer ND, Manning DK, Bjork BC, Li C, Montgomery K, Siepka SM, Vitaterna MH, Takahashi JS, Wiltshire T, Kwiatkowski DJ, Kucherlapati R, Beier DR. Utilization of a whole genome SNP panel for efficient genetic mapping in the mouse. *Genome Res* 2006;16:436–440.
17. Arends D, Prins P, Jansen RC, Broman KW. R/QTL: high-throughput multiple QTL mapping. *Bioinformatics* 2010;26: 2990–2992.
18. Smith R, Sheppard K, Dipetrillo K, Churchill G. Quantitative trait locus analysis using J/qtl. *Methods Mol Biol* 2009;753: 175–188.
19. Le Voyer T, Rouse J, Lu Z, Lifsted T, Williams M, Hunter KW. Three loci modify growth of a transgene-induced mammary tumor: suppression of proliferation associated with decreased microvessel density. *Genomics* 2001;74:253–261.
20. Rogers MS, Rohan RM, Birsner AE, D'Amato RJ. Genetic loci that control vascular endothelial growth factor-induced angiogenesis. *FASEB J* 2003;17:2112–2114.
21. Carter MG, Sharov AA, VanBuren V, Dudekula DB, Carmack CE, Nelson C, Ko MS. Transcript copy number estimation using a mouse whole-genome oligonucleotide microarray. *Genome Biol* 2005;6:R61.
22. Benzinou M, Clermont FF, Letteboer TG, Kim JH, Espejel S, Harradine KA, Arbelaez J, Luu MT, Roy R, Quigley D, Higgins MN, Zaid M, Aouizerat BE, van Amstel JK, Giraud S, Dupuis-Girod S, Lesca G, Plauchu H, Hughes CC, Westermann CJ, Akhurst RJ. Mouse and human strategies identify PTPN14 as a modifier of angiogenesis and hereditary haemorrhagic telangiectasia. *Nat Commun* 2012;3:616.
23. Rogers MS, Boyartchuk V, Rohan RM, Birsner AE, Dietrich WF, D'Amato RJ. The classical pink-eyed dilution mutation affects angiogenic responsiveness. *PLoS ONE* 2012;7:e35237.
24. Debette S, Visvikis-Siest S, Chen MH, Ndiaye NC, Song C, Destefano A, Safa R, Azimi Nezhad M, Sawyer D, Marteau JB, Xanthakis V, Siest G, Sullivan L, Pfister M, Smith H, Choi SH, Lamont J, Lind L, Yang Q, Fitzgerald P, Ingelsson E, Vasan RS, Seshadri S. Identification of cis- and trans-acting genetic variants explaining up to half the variation in circulating vascular endothelial growth factor levels. *Circ Res* 2011;109:554–563.
25. Sillén A, Brohede J, Lilius L, Forsell C, Andrade J, Odeberg J, Ebise H, Winblad B, Graff C. Linkage to 20p13 including the ANGPT4 gene in families with mixed Alzheimer's disease and vascular dementia. *J Hum Genet* 2010;55:649–655.
26. Ferlini A, Bovolenta M, Neri M, Gualandi F, Balboni A, Yuryev A, Salvi F, Gemmati D, Liboni A, Zamboni P. Custom CGH array profiling of copy number variations (CNVs) on chromosome 6p21.32 (HLA locus) in patients with venous malformations associated with multiple sclerosis. *BMC Med Genet* 2010;11:64.
27. Herzog W, Müller K, Huisken J, Stainier DY. Genetic evidence for a noncanonical function of seryl-tRNA synthetase in vascular development. *Circ Res* 2009;104:1260–1266.
28. Carmeliet P, Ferreira V, Breier G, Pollefeyt S, Kieckens L, Gertsenstein M, Fahrig M, Vandenhoeck A, Harpal K, Eberhardt C, Declercq C, Pawling J, Moons L, Collen D, Risau W, Nagy A. Abnormal blood vessel development and lethality in embryos lacking a single VEGF allele. *Nature* 1996; 380:435–439.
29. Zhang XQ, Takakura N, Oike Y, Inada T, Gale NW, Yancopoulos GD, Suda T. Stromal cells expressing ephrin-B2 promote the growth and sprouting of ephrin-B2(+) endothelial cells. *Blood* 2001;98:1028–1037.
30. Zhong TP, Childs S, Leu JP, Fishman MC. Gridlock signalling pathway fashions the first embryonic artery. *Nature* 2001;414: 216–220.
31. Droin N, Hendra JB, Ducoroy P, Solary E. Human defensins as cancer biomarkers and antitumour molecules. *J Proteomics* 2009;72:918–927.
32. Economopoulou M, Bdeir K, Cines DB, Fogt F, Bdeir Y, Lubkowski J, Lu W, Preissner KT, Hammes HP, Chavakis T. Inhibition of pathologic retinal neovascularization by alpha-defensins. *Blood* 2005;106:3831–3838.
33. Stappenbeck TS, Hooper LV, Gordon JI. Developmental regulation of intestinal angiogenesis by indigenous microbes via Paneth cells. *Proc Natl Acad Sci USA* 2002;99:15451–15455.